Metal–metal interactions across bridging elemental carbon chains: a computational study of odd-carbon complexes†

Haijun Jiao and John A. Gladysz*

Institut für Organische Chemie, Friedrich-Alexander Universität Erlangen-Nürnberg, Henkestrasse 42, 91054 Erlangen, Germany. E-mail: gladysz@organik.uni-erlangen.de

Received (in Montpellier, France) 31st October 2000, Accepted 22nd January 2001

Structure, bonding and metal–metal interactions in complexes $[L_yMC_xM'L'_{y'}]^{z+}$ with odd-carbon chains, and monometallic reference compounds, are investigated at the B3LYP density functional level of theory. The data show strong rhenium–manganese interactions in $[(\eta^5\text{-}C_5H_5)(NO)(PH_3)ReC_xMn(CO)_2(\eta^5\text{-}C_5H_5)]^+$ ($x = 3, 5, 7, 9$), as evidenced by bond lengths and orders, charge distributions, and negative homodesmotic energies (which diminish with chain length). Natural bond orbital (NBO) analyses give ground states with highly polarized Re–C bonds, and suggest dominant $^+Re\text{–}(C{=}C)_n{=}C{=}Mn$ as opposed to $^+Re{=}(C{=}C)_n{=}C{=}Mn$ character. The corresponding dirhenium complexes are similar but with dominant $Re(\text{–}C{\equiv}C)_n\text{–}C{\equiv}Re^+$ character. The more symmetrical uncharged complexes $(\eta^5\text{-}C_5H_5)(CO)_2M(1)C_xM(2)(CO)_2(\eta^5\text{-}C_5H_5)$ [$x = 3, 5$; M(1), M(2) = Re or Mn] exhibit analogous geometric, electronic and homodesmotic energy trends, but have dominant $M{=}(C{=}C)_n{=}C{=}M$ character. In contrast, $(\eta^5\text{-}C_5H_5)(NO)(PH_3)ReC_3W(OMe)_3$ which has a $ReC{\equiv}CC{\equiv}W$ linkage, shows no significant (net) rhenium–tungsten interactions. All geometric and electronic properties are very close to those of monometallic reference compounds. Homodesmotic energies are near zero, although related triple bond metatheses used preparatively are exothermic. The dimerization of $(MeO)_3W{\equiv}CH$ is exothermic (-14.6 kcal mol^{-1}), giving a methoxy-bridged structure closely resembling literature compounds.

One of the most exciting interfaces of organic, inorganic and materials chemistry involves complexes in which sp carbon chains span two transition metals, $[L_yMC_xM'L'_{y'}]^{z+}$ (**I**).[1] Such species exhibit a wealth of fascinating physical and chemical properties, which can be studied as a function of oxidation state and chain length.[2–7] Different oxidation states are usually characterized by different valence states, such as $[L_yM(\text{–}C{\equiv}C)_n\text{–}M'L'_{y'}]^{z+}$, $[L_yM(=C{=}C)_n{=}M'L'_{y'}]^{(z+2)+}$ and $[L_yM(\equiv C\text{–}C)_n{\equiv}M'L'_{y'}]^{(z+4)+}$ for even-carbon chains. The first and third represent polyyne motifs, and the second a cumulenic motif. Each oxidation state presents further questions, such as the dominant resonance structure and nature of excited states. The resonance structure or ground state favored at chain length C_x is not necessarily the same at chain length C_{2x}. Oxidation states with odd electrons present additional structure and bonding issues, such as the extent of delocalization between metal termini.[1,2b,e,3,4,7h]

Such a complex array of questions can only be addressed through detailed experimental and computational studies. In an earlier collaboration with Frenking, we modeled the structural and electronic properties of the neutral and dicationic dirhenium C_4 complexes $(\eta^5\text{-}C_5Me_5)(NO)(PPh_3)\text{-}Re(C{\equiv}CC{\equiv}C)Re(PPh_3)(NO)(\eta^5\text{-}C_5Me_5)$ (**1**) and $[(\eta^5\text{-}C_5Me_5)\text{-}(NO)(PPh_3)Re(=C{=}C{=}C{=}C{=})Re(PPh_3)(NO)(\eta^5\text{-}C_5Me_5)]^{2+}$ $2PF_6^-$ ($\mathbf{1}^{2+}2PF_6^-$) at the Hartree–Fock (HF) level. However, the isolable intermediate radical cation did not give SCF convergence.[2b] Other experimental/computational partnerships include the Halet and Bruce groups [diruthenium[4b] and di(tris-metal) cluster[8] complexes] and the Sgamellotti and Floriani groups.[9] In one paper,[9c] the latter team treated many of the dirhenium and diiron systems of particular interest to us and the Lapinte group.[2,3,7h] Naturally, there is a much wider body of theoretical work concerned with C_x fragments, monomeric carbon allotropes, and various metal adducts thereof.[10]

We sought to build a firm computational foundation to systematically address the types of issues outlined above, starting with complexes containing at least one chiral rhenium endgroup of the formula $(\eta^5\text{-}C_5H_5)(NO)(PH_3)Re$. Hence, we have initiated a program of high level B3LYP density functional calculations. Our first paper in this series, involving simple model complexes of the type $[(\eta^5\text{-}C_5H_5)(NO)(PR_3)ReCH_3]^{n+}nX^-$ ($\mathbf{2}^{n+}nX^-$; $n = 0$, 1; R = H, CH_3) and $[(\eta^5\text{-}C_5H_5)(NO)(PR_3)Re{=}CH_2]^+X^-$ ($\mathbf{3}^+X^-$; R = H, CH_3), has just appeared.[11] A much more extensive paper involving dirhenium complexes with even-carbon chains ($\mathbf{1}^{n+}nPF_6^-$ and higher homologs) is in preparation.[12] In this paper, we treat complexes with odd-carbon chains. These can adopt two types of valence structures, as illustrated in Scheme 1: the cumulenic form **Ia** or the polyynyl/carbyne form **Ib**.

Curiously, relatively few complexes of the type **I** with odd-carbon chains are known. Outside of C_1 complexes, there are only a handful,[2d,5,6] examples, some of which are given in Scheme 2. We have prepared a family of cumulated rhenium/manganese and rhenium/iron C_3 complexes of the formula $[(\eta^5\text{-}C_5Me_5)(NO)(PPh_3)Re(=C{=}C{=}C{=})M(CO)_a(\eta^5\text{-}C_5H_cCl_{5-c})_b]^+BF_4^-$ ($M/a/b/c$ = Mn/2/1/5, $\mathbf{4}^+BF_4^-$; Mn/2/1/4; Mn/2/1/0/; Fe/4/0/ –), and one labile rhenium/manganese C_5 homolog $[(\eta^5\text{-}C_5Me_5)(NO)(PPh_3)Re(=C{=}C{=}C{=}C{=}C{=})Mn\text{-}(CO)_2(\eta^5\text{-}C_5Cl_5)]^+BF_4^-$.[2d] Woodward and Templeton have reported labile group 6 cumulated systems, such as $(K^+)_2$

$[L_yM{=}C{=}C{\frac{}{}}_nC{=}M'L_{y'}]^{z+}$ (Ia) $[L_yM(\text{–}C{\equiv}C)_n\text{–}C{\equiv}M'L_{y'}]^{z+}$ (Ib)

Scheme 1 Two valence structures for odd-carbon complexes $[L_yMC_xM'L_{y'}]^{z+}$ (**I**).

† Dedicated to Prof. Dr Paul von Ragué Schleyer on the occasion of his 71st birthday.

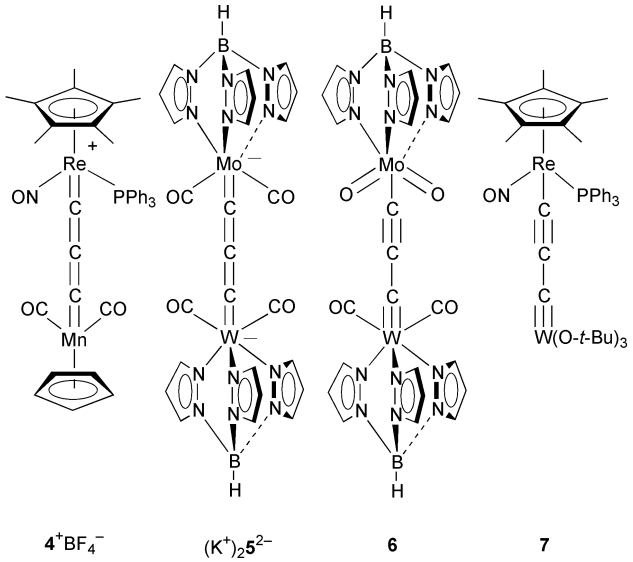

Scheme 2 Representative C_3 complexes of type **I**.

$[Tp'(CO)_2Mo(=C=C=C=)W(CO)_2Tp']^{2-}$ $[(K^+)_2\mathbf{5}^{2-}]$, which can be oxidized to isolable alkynyl/carbyne species, such as $Tp'(O)_2Mo(C{\equiv}CC{\equiv})W(CO)_2Tp'$ (**6**).[5] More recently, we isolated the alkynyl/carbyne complex $(\eta^5\text{-}C_5Me_5)$-$(NO)(PPh_3)Re(C{\equiv}CC{\equiv})W(O\text{-}t\text{-}Bu)_3$ (**7**).[6] Complexes with other types of C_3 ligands have also been reported.[1,3] Although stable type **I** complexes with quite long even-numbered polyynediyl chains are known (C_{12}, C_{16}, C_{20}),[2e,7b,c] available data suggest that the kinetic stabilities of the odd-carbon systems decrease more dramatically with increasing chain length.

In this paper, we describe a computational study of structure, bonding, and metal–metal interactions in all classes of C_3 complexes for which structural data are available ($\mathbf{4}^+BF_4^-$, **7**), and higher C_5, C_7 and C_9 homologs. Several presently unknown families are also investigated. These represent the first computational data of any type for type **I** complexes with odd-carbon chains. Our results help to address many of the questions outlined above and provide a number of useful predictions for future experimental investigations.

Computational methods

Calculations were carried out at the B3LYP level of density functional theory as implemented in the GAUSSIAN 98 program.[14] Both the LANL2DZ and LANL2DZp (with a set of polarization function) basis sets[15] were used for geometry optimizations of C_3 complexes and fragments derived therefrom. The B3LYP/LANL2DZ combination was used for the C_3 frequency calculations and geometry optimizations of longer C_x species (due to the dramatically higher computer resources required). For the same reason, $\eta^5\text{-}C_5Me_5$, PPh_3 and O-*t*-Bu were modeled with smaller $\eta^5\text{-}C_5H_5$, PH_3 and OCH_3 ligands. NBO (natural bond orbital) analyses were used to characterize bonding and charge distributions.[16] The calculated total electronic energies are summarized in Table 1.

Table 1 Computed total energies E_{tot} (au)

Compound	E_{tot} [a]	E_{tot} [b]
$(\eta^5\text{-}C_5H_5)(CO)_2MnC_3H_2$ (**MnC$_3$H$_2$**)	−639.478 87	−639.637 28
$(\eta^5\text{-}C_5H_5)(CO)_2MnC_3$ (**MnC$_3$**)		−638.363 43
$[(\eta^5\text{-}C_5H_5)(NO)(PH_3)ReC_3H_2]^+$ ($[$**ReC$_3$H$_2$**$]^+$)	−526.044 64	−526.199 49
$[(\eta^5\text{-}C_5H_5)(CO)_2MnC_3Re(PH_3)(NO)(\eta^5\text{-}C_5H_5)]^+$ (**8**$^+$)	−1048.915 16	−1049.211 27
$H_2C_3H_2$	−116.640 70	−116.661 31
$(\eta^5\text{-}C_5H_5)(CO)_2MnC_5H_2$ (**MnC$_5$H$_2$**)	−715.623 41	−715.795 84
$[(\eta^5\text{-}C_5H_5)(NO)(PH_3)ReC_5H_2]^+$ ($[$**ReC$_5$H$_2$**$]^+$)	−602.190 36	−602.358 97
$[(\eta^5\text{-}C_5H_5)(CO)_2MnC_5Re(PH_3)(NO)(\eta^5\text{-}C_5H_5)]^+$ (**9**$^+$)	−1125.060 36	
$H_2C_5H_2$	−192.775 68	−192.810 45
$(\eta^5\text{-}C_5H_5)(CO)_2MnC_7H_2$ (**MnC$_7$H$_2$**)	−791.768 33	−791.954 76
$[(\eta^5\text{-}C_5H_5)(NO)(PH_3)ReC_7H_2]^+$ ($[$**ReC$_7$H$_2$**$]^+$)	−678.336 92	−678.519 14
$[(\eta^5\text{-}C_5H_5)(CO)_2MnC_7Re(PH_3)(NO)(\eta^5\text{-}C_5H_5)]^+$ (**10**$^+$)	−1201.206 55	
$H_2C_7H_2$	−268.916 47	−268.965 08
$(\eta^5\text{-}C_5H_5)(CO)_2MnC_9H_2$ (**MnC$_9$H$_2$**)	−867.913 41	
$[(\eta^5\text{-}C_5H_5)(NO)(PH_3)ReC_9H_2]^+$ ($[$**ReC$_9$H$_2$**$]^+$)	−754.483 58	
$[(\eta^5\text{-}C_5H_5)(CO)_2MnC_9Re(PH_3)(NO)(\eta^5\text{-}C_5H_5)]^+$ (**11**$^+$)	−1277.352 68	
$H_2C_9H_2$	−345.059 27	
$(\eta^5\text{-}C_5H_5)(CO)_2ReC_3H_2$ (**Re′C$_3$H$_2$**)	−614.720 44	−614.876 54
$(\eta^5\text{-}C_5H_5)(CO)_2ReC_3Re(CO)_2(\eta^5\text{-}C_5H_5)$ (**12**)	−1112.836 28	−1113.127 16
$(\eta^5\text{-}C_5H_5)(CO)_2MnC_3Mn(CO)_2(\eta^5\text{-}C_5H_5)$ (**13**)	−1162.352 26	−1162.647 40
$(\eta^5\text{-}C_5H_5)(CO)_2ReC_3Mn(CO)_2(\eta^5\text{-}C_5H_5)$ (**14**)	−1137.594 59	−1137.887 36
$[(\eta^5\text{-}C_5H_5)(CO)_2ReC_3Re(PH_3)(NO)(\eta^5\text{-}C_5H_5)]^+$ (**15**$^+$)	−1024.160 85	−1024.454 39
$(\eta^5\text{-}C_5H_5)(CO)_2ReC_5H_2$ (**Re′C$_5$H$_2$**)	−690.865 24	−691.035 40
$(\eta^5\text{-}C_5H_5)(CO)_2ReC_5Re(CO)_2(\eta^5\text{-}C_5H_5)$ (**16**)	−1188.977 73	
$(\eta^5\text{-}C_5H_5)(CO)_2MnC_5Mn(CO)_2(\eta^5\text{-}C_5H_5)$ (**17**)	−1238.493 23	
$(\eta^5\text{-}C_5H_5)(CO)_2ReC_5Mn(CO)_2(\eta^5\text{-}C_5H_5)$ (**18**)	−1213.735 74	
$[(\eta^5\text{-}C_5H_5)(CO)_2ReC_5Re(PH_3)(NO)(\eta^5\text{-}C_5H_5)]^+$ (**19**$^+$)	−1100.306 23	
$(\eta^5\text{-}C_5H_5)(NO)(PH_3)ReC{\equiv}CC{\equiv}W(OMe)_3$ (**21**)		−938.595 45
$(MeO)_3W{\equiv}W(OMe)_3$ (**22**)		−826.750 38
$(\eta^5\text{-}C_5H_5)(NO)(PH_3)ReC{\equiv}CC{\equiv}CH$ (**23**)		−563.873 37
$(\eta^5\text{-}C_5H_5)(NO)(PH_3)ReC{\equiv}CC{\equiv}CMe$ (**24**)		−603.202 66
$(MeO)_3W{\equiv}CH$ (**25**)[c]		−452.046 09
$(MeO)_3W{\equiv}CMe$ (**26**)		−491.371 26
$(MeO)_3W{\equiv}CC{\equiv}CH$ (**27**)		−528.209 23
$(MeO)_3W{\equiv}CC{\equiv}CMe$ (**28**)		−567.536 92
$[(MeO)_3W{\equiv}CH]_2$ (**29**)[c]		−904.117 91
$HC{\equiv}CC{\equiv}CH$		−153.484 82
$MeC{\equiv}CC{\equiv}CMe$		−232.144 15

[a] At B3LYP/LANL2DZ. [b] At B3LYP/LANL2DZp. [c] The ZPE (kcal mol^{-1}, B3LYP/LANL2DZ) is 177.7 for **29** and 88.0 for **25**.

Results and discussion

Structures of ReC_xMn systems and fragments thereof

The structure of the model compound $[(\eta^5\text{-}C_5H_5)(NO)(PH_3)ReC_3Mn(CO)_2(\eta^5\text{-}C_5H_5)]^+$ (**8**$^+$) was studied first. As shown in Fig. 1, the optimized bond lengths and angles (in bold) at the B3LYP/LANL2DZp level agree well with the X-ray data (in italics) for the closely related molecule **4**$^+BF_4^-$.[2d] The latter exhibits two independent cations in the unit cell and so metrical parameters are given as ranges. The linearity of the ReCCCMn unit is indicated by the MnCC (179.7°), ReCC (176.0°) and CCC (175.9°) bond angles. At the same level, the C=C bond lengths are 1.321 and 1.277 Å. The Re–C bond (1.941 Å) is somewhat longer than that calculated for the reference vinylidene complex $[(\eta^5\text{-}C_5H_5)(NO)(PH_3)Re{=}C{=}CH_2]^+$ (1.897 Å), but shorter than that of the ethynyl complex $(\eta^5\text{-}C_5H_5)(NO)(PH_3)ReC{\equiv}CH$ (2.042 Å).[12,17] The distance between the heavy rhenium and manganese atoms in **4**$^+BF_4^-$ is very accurately determined by the X-ray data (6.249–6.241 Å) and the computed distance for **8**$^+$ is in perfect agreement (6.246 Å). The computations also reproduce the *cis* relationship of the manganese–C_5R_5-centroid vector and the Re–P bond (torsion type angle 2.1 *vs.* 7.9–0.1°).

This conformation can be rationalized from the frontier molecular orbitals of the formally octahedral metal endgroups, analogous to the way in which perpendicular $=CR_2$ orientations are predicted for pentatetraenes ($R_2C{=}C{=}C{=}C{=}CR_2$). As shown in Fig. 2(A), the $[(\eta^5\text{-}C_5H_5)(NO)(PH_3)Re]^+$ fragment HOMO has mainly metal-d character. The plane of the four lobes contains the Re–P bond, which runs along a node. The $(\eta^5\text{-}C_5H_5)(CO)_2Mn$ fragment HOMO is also metal-d type [Fig. 2(B)], with the plane of the four lobes approximately parallel to that of the cyclopentadienyl ligand. The π bonding orbitals at opposite ends of the =C=C=C= bridges are orthogonal. As illustrated in Fig. 2(C), overlap gives the relative endgroup conformations shown in Fig. 1.

In order to further define the geometric consequences of metal–metal interaction and charge transfer in **8**$^+$ and

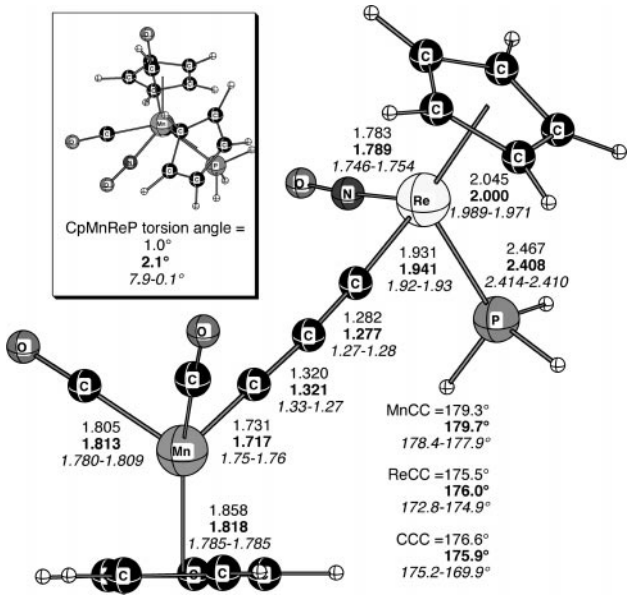

Fig. 1 Computed bond lengths (Å) and angles (deg) for $[(\eta^5\text{-}C_5\underline{H}_5)(NO)(P\underline{H}_3)ReC_3Mn(CO)_2(\eta^5\text{-}C_5H_5)]^+$ (**8**$^+$; B3LYP/LANL2DZ in plain text and B3LYP/LANL2DZp in bold), compared to the X-ray data for $[(\eta^5\text{-}C_5\underline{Me}_5)(NO)(P\underline{Ph}_3)Re{=}C{=}C{=}C{=}Mn(CO)_2(\eta^5\text{-}C_5H_5)]^+BF_4^-$ (**4**$^+BF_4^-$; italics).

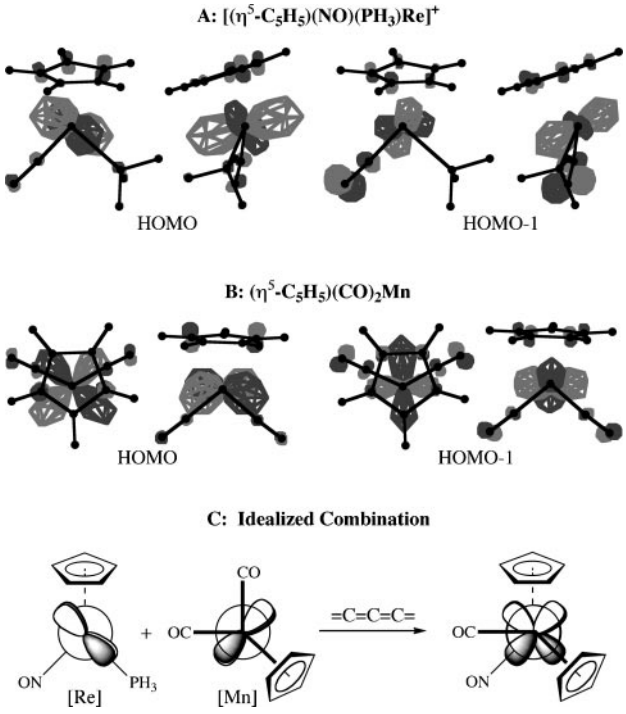

Fig. 2 Frontier molecular orbitals of metal endgroup fragments.

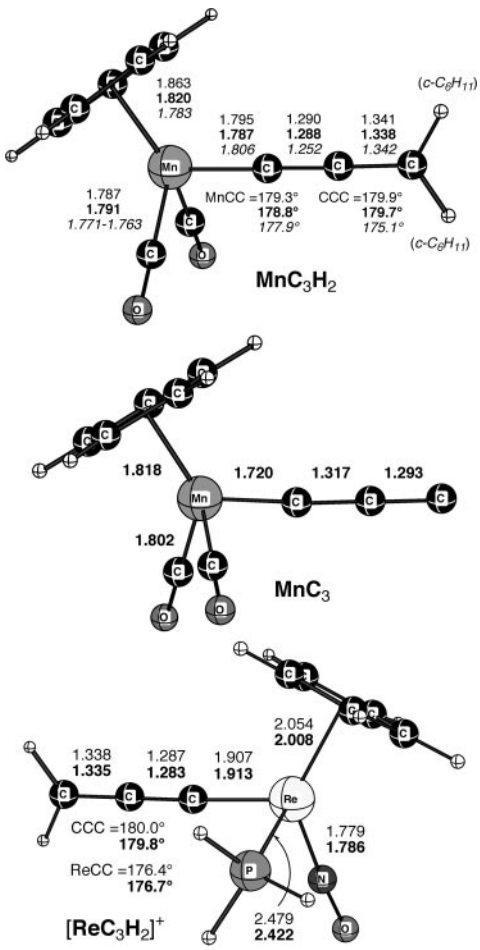

Fig. 3 Computed bond lengths (Å) and angles (deg) for the monometallic complexes $(\eta^5\text{-}C_5H_5)(CO)_2MnC_3H_2$ (**MnC$_3$H$_2$**), $(\eta^5\text{-}C_5H_5)(CO)_2MnCCC$: (**MnC$_3$**) and $[(\eta^5\text{-}C_5H_5)(NO)(PH_3)ReC_3H_2]^+$ (**[ReC$_3$H$_2$]$^+$**) (B3LYP/LANL2DZ in plain text and B3LYP/LANL2DZp in bold) and a comparison to the X-ray data for $(\eta^5\text{-}C_5H_5)(CO)_2MnC_3(c\text{-}C_6H_{11})_2$ (italics).

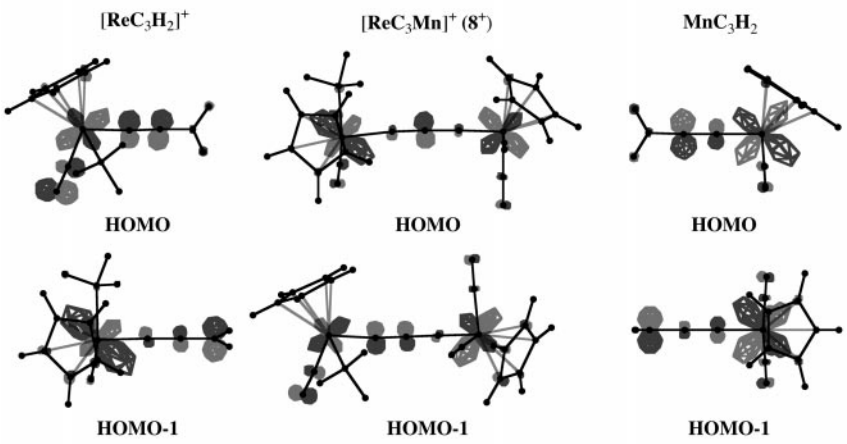

Fig. 4 Frontier molecular orbitals of model complexes.

$\mathbf{4}^{+}BF_4^{-}$, monometallic reference compounds were studied. Fig. 3 summarizes the optimized data for allenylidene complexes $[(\eta^5\text{-}C_5H_5)(NO)(PH_3)Re{=}C{=}C{=}CH_2]^+$ ($[\mathbf{ReC_3H_2}]^+$) and $[(\eta^5\text{-}C_5H_5)(CO)_2Mn{=}C{=}C{=}CH_2]$ ($\mathbf{MnC_3H_2}$). No crystallographic data are yet available for monorhenium analogs of $[\mathbf{ReC_3H_2}]^+$, although the dirhenium $^{+}Re{=}C{=}C{=}C{=}C{=}Re^{+}$ species $\mathbf{1}^{2+}2PF_6^{-}$ has been structurally characterized.[2b] The optimized geometry for $\mathbf{MnC_3H_2}$ is close to that of the di(cyclohexyl)propadienylidene complex $(\eta^5\text{-}C_5H_5)(CO)_2Mn{=}C{=}C{=}C(c\text{-}C_6H_{11})_2$,[18] data for which are also presented in Fig. 3.

As shown in Fig. 3, the plane of the $=CH_2$ group is nearly perpendicular to the Re–P bond in $[\mathbf{ReC_3H_2}]^+$ and bisects the cyclopentadienyl ring in $\mathbf{MnC_3H_2}$. These conformations follow logically from the frontier molecular orbitals of the endgroups (Fig. 2). The highest occupied molecular orbitals of all of these C_3 systems are summarized in Fig. 4.

In order to define the effect of chain length upon molecular properties, higher C_5 ($\mathbf{9}^+$), C_7 ($\mathbf{10}^+$) and C_9 ($\mathbf{11}^+$) homologs of $\mathbf{8}^+$ were investigated. The corresponding monometallic complexes, $[\mathbf{ReC_xH_2}]^+$ and $\mathbf{MnC_xH_2}$, were similarly studied. Due to the massive computer resources required, the bimetallic complexes were optimized only at the B3LYP/LANL2DZ level. Key parameters are summarized in Fig. 5. The structures of the metal fragments are essentially unchanged from those in Fig. 1 and 3. No crystallographic data are currently available for closely related compounds. However, several pentatetraenylidene complexes, $[L_nM{=}C{=}C{=}C{=}CR_2]^{z+}$ have been isolated,[19,20] and three crystal structures have been reported.[20] These represent the longest structurally characterized metallacumulenes in the literature.

Structural evidence for metal–metal interactions in ReC_xMn systems

At the B3LYP/LANL2DZp level, the Re–C and Mn–C bonds of $\mathbf{8}^+$ (1.941, 1.717 Å) are longer and shorter, respectively, than those of the corresponding monometallic allenylidene complexes $[\mathbf{ReC_3H_2}]^+$ and $\mathbf{MnC_3H_2}$ (1.913, 1.787 Å). On the other hand, the ReC=C and MnC=C bonds in $\mathbf{8}^+$ (1.277, 1.321 Å) are shorter and longer than those in the monometallic reference complexes (1.283, 1.288 Å). These substantial differences must in some way be derived from metal–metal interactions. They indicate that the Re–C bond in $\mathbf{8}^+$ is weaker, and the Mn–C bond stronger, than in the monometallic complexes.

In order to better interpret the M–C bond length trends, NBO and charge analyses were conducted, as summarized in Table 2. The data show that electrostatic polarization effects play a key role. Specifically, the difference in natural charge

Table 2 Natural charge, bond hybridization (orbital coefficients) and NLMO bond order data (B3LYP/LANL2DZp)

	$\mathbf{8}^+$ ($[\mathbf{ReC_3Mn}]^+$)	$[\mathbf{ReC_3H_2}]^+$	$\mathbf{MnC_3H_2}$	$\mathbf{MnC_3}$
Natural charge				
$^{\delta}M$	0.810/Re[a]	0.976/Re[a]		
	0.225/Mn[b]		0.013/Mn[b]	−0.060/Mn[b]
$\Delta(^{\delta}M - {}^{\delta}C)$[c]	0.227/Re–C	0.396/Re–C		
	0.764/Mn–C		0.545/Mn–C	0.871/Mn–C
Hybridization (orbital coefficients)				
M–C/σ	$s^1d^{8.95}$ (Re, 37.2%)	$s^1d^{8.96}$ (Re, 38.8%)		
	$s^1p^{1.02}$ (CRe, 61.4%)	$s^1p^{1.04}$ (CRe, 60.0%)		
	$s^1d^{6.77}$ (Mn, 35.3%)		$s^1d^{6.93}$ (Mn, 34.7%)	$s^1d^{6.95}$ (Mn, 36.2%)
	$s^1p^{0.83}$ (CMn, 61.0%)		$s^1p^{0.88}$ (CMn, 61.3%)	$s^1p^{0.84}$ (CMn, 60.0%)
M–C/π	d (Mn, 66.8%)	d (Re, 69.3%)	d (Mn, 66.5%)	d (Mn, 73.2%)
	p (CMn, 23.9%)	p (CRe, 23.8%)	p (CMn, 22.3%)	p (CMn, 18.3%)
Lone pair	d (Re, 81.0%)[d]			
interactions	p (CRe, 10.0%)			
	d (Mn, 82.6%)[e]			d (Mn, 81.5%)[f]
	p (CMn, 7.3%)			p (CMn, 7.7%)
NLMO	0.852/Re–C	1.099/Re–C		
bond order	1.075/Mn–C		0.962/Mn–C	1.010/Mn–C

[a] The $(\eta^5\text{-}C_5H_5)(NO)(PH_3)Re$ endgroup. [b] The $(\eta^5\text{-}C_5H_5)(CO)_2Mn$ endgroup. [c] The charge difference between metal and the first chain carbon. [d] d-Type lone pair on rhenium with partial occupation of 1.64 electrons. [e] d-Type lone pair on manganese with partial occupation of 1.67 electrons. [f] d-Type lone pair on manganese with partial occupation of 1.63 electrons.

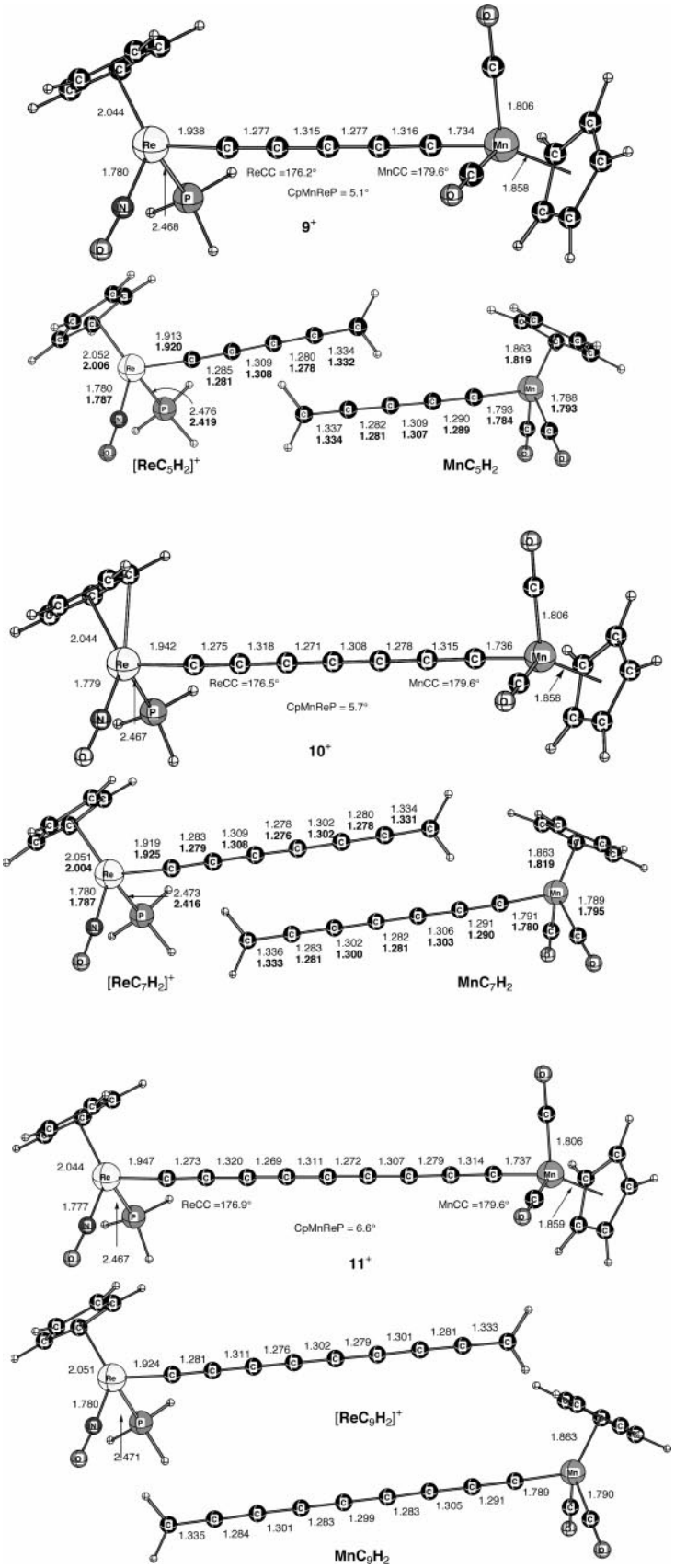

Fig. 5 Computed bond lengths (Å) and angles (deg) for $[(\eta^5\text{-}C_5H_5)(NO)(PH_3)ReC_xMn(CO)_2(\eta^5\text{-}C_5H_5)]^+$ ($x = 5$, $\mathbf{9}^+$; 7, $\mathbf{10}^+$; 9, $\mathbf{11}^+$) and the monometallic reference molecules $[(\eta^5\text{-}C_5H_5)(NO)(PH_3)ReC_xH_2]^+$ ($[\mathbf{ReC}_x\mathbf{H}_2]^+$) and $(\eta^5\text{-}C_5H_5)(CO)_2MnC_xH_2$ ($\mathbf{MnC}_x\mathbf{H}_2$) (B3LYP/LANL2DZ in plain text and B3LYP/LANL2DZp in bold).

between the manganese and carbon atoms in $\mathbf{8}^+$ (0.764) is larger than that in $\mathbf{MnC_3H_2}$ (0.545). In contrast, the difference in natural charge between the rhenium and carbon atoms in $\mathbf{8}^+$ (0.227) is smaller than that in $[\mathbf{ReC_3H_2}]^+$ (0.396). These trends are also reflected in the NLMO bond orders (Table 2). Specifically, the Mn–C value in $\mathbf{8}^+$ (1.075) is greater than that in $\mathbf{MnC_3H_2}$ (0.962), while the Re–C value in $\mathbf{8}^+$ (0.852) is less than that in $[\mathbf{ReC_3H_2}]^+$ (1.099). The partial bond orders are

the result of highly polarized bonding orbitals and slightly occupied antibonding orbitals.

The metal–carbon hybridization data also provide insights. First, note that the representative reference compound $[\mathbf{ReC_3H_2}]^+$ has a Re–C σ bond comprised of a $s^1p^{1.04}$ carbon orbital and a $s^1d^{8.96}$ rhenium orbital, and a Re–C π bond comprised of a pure p carbon orbital and a pure d rhenium orbital. The corresponding orbital coefficients feature significant contributions from both atoms (>22% for carbon). Therefore $[\mathbf{ReC_3H_2}]^+$, and for analogous reasons $\mathbf{MnC_3H_2}$, have dominant M=C double bond character. The bimetallic complex $\mathbf{8}^+$ similarly has a Mn=C double bond, and the orbitals and coefficients for the Re–C σ bond are essentially identical to those of $[\mathbf{ReC_3H_2}]^+$. However, the other set of rhenium–carbon orbital coefficients features only a small contribution from carbon (10.0%). Accordingly, the program output indicates dominant Re–C single bond character and a largely localized rhenium d-type lone pair with a partial occupation of 1.64 electrons. It interacts only slightly with the ligating carbon atom.

This largely localized lone pair has a counterpart on manganese that becomes important in other contexts below. It is orthogonal to the fragment HOMO in Fig. 2 and has a partial occupation of 1.67 electrons. There is little, if any, Mn≡C triple bond character, as indicated by the small coefficient of the respective carbon p orbital (7.3%). The reference compound $\mathbf{MnC_3H_2}$ has an analogous lone pair, which interacts slightly with the carbonyl ligands, consistent with its shorter Mn–C(O) bond length (1.791 *vs.* 1.813 Å). Regardless, according to NBO analysis, the model compound $\mathbf{8}^+$ is best described as an adduct of the neutral singlet carbene $(\eta^5\text{-}C_5H_5)(CO)_2Mn{=}C{=}C{=}C{:}$ ($\mathbf{MnC_3}$) and the positive $[(\eta^5\text{-}C_5H_5)(NO)(PH_3)Re]^+$ fragment. This is further evidenced by the close similarities of the Mn–C bond lengths and orders for $\mathbf{MnC_3}$ and $\mathbf{8}^+$ (1.720 *vs.* 1.717 Å and 1.010 *vs.* 1.075 Å; Fig. 3 and Table 2), as well as the C=C bond lengths, which differ from those of $\mathbf{MnC_3H_2}$ (1.317 and 1.321 *vs.* 1.288 Å; 1.293 and 1.277 *vs.* 1.338 Å).

Charge transfer is reflected by the calculated natural charges. Not surprisingly, the rhenium fragment in $[\mathbf{ReC_3H_2}]^+$ bears nearly all the positive charge (0.976), while the manganese fragment in $\mathbf{MnC_3H_2}$ is neutral (0.013). In $\mathbf{8}^+$, the rhenium fragment is less positively charged (0.810) and the manganese fragment has a slight positive charge (0.225). This can be viewed as a ground state charge transfer of magnitude 0.166 from rhenium to manganese through the C_3 chain. Since the sum of these natural charges is very close to the charge of the complex (unity), there is essentially no net charge associated with the chain.

Fig. 5 shows that when the carbon chain in $\mathbf{8}^+$ is extended, the M–C bond distances increase monotonically. Upon going from $\mathbf{8}^+$ to $\mathbf{11}^+$, the Mn–C bond lengthens (at the B3LYP/LANL2DZ level) from 1.731 to 1.737 Å. At the same time, the Re–C bond lengthens from 1.931 to 1.947 Å. Thus, the bond orders at both metal termini decrease. The monorhenium reference compounds behave similarly (from $[\mathbf{ReC_3H_2}]^+$ to $[\mathbf{ReC_9H_2}]^+$, 1.907 to 1.924 Å). However, the Mn–C bonds of the monomanganese compounds contract slightly as the chains are extended (from $\mathbf{MnC_3H_2}$ to $\mathbf{MnC_9H_2}$, 1.795 to 1.789 Å). Regardless, the higher ReC_xMn complexes $\mathbf{9}^+$ and $\mathbf{11}^+$ are similar with respect to all of the properties analyzed above.

Hence, when the model compounds $\mathbf{8}^+$–$\mathbf{11}^+$ are viewed by the NBO formalism, the general formulation $^+Re{-}(C{=}C)_n{=}C{=}Mn$, with a highly polarized rhenium carbon bond, best describes the ground states. The cumulenic formulation $^+Re{=}(C{=}C)_n{=}C{=}Mn$ represents the next most important resonance structure. As illustrated in Fig. 2, this resonance structure is conformation-determining. Hence, we continue to draw the parent molecule $\mathbf{4}^+BF_4^-$ as fully cumulated, as shown in Scheme 2. It is also worth noting that the donor properties of pentamethylcyclopentadienyl metal fragments are commonly greater than those of cyclopentadienyl analogs.

$$MnC_xH_2 + [ReC_xH_2]^+ = H_2C_xH_2 + [(\eta^5\text{-}C_5H_5)(NO)(PH_3)ReC_xMn(CO)_2(\eta^5\text{-}C_5H_5)]^+$$

$\Delta H = -\mathbf{22.5}/-20.3$ ($\mathbf{8}^+$, $x = 3$)
$\Delta H = -14.0$ ($\mathbf{9}^+$, $x = 5$)
$\Delta H = -11.2$ ($\mathbf{10}^+$, $x = 7$)
$\Delta H = -9.4$ ($\mathbf{11}^+$, $x = 9$)

Scheme 3 Homodesmotic energies (kcal mon^{-1}) for $\mathbf{8}^+$–$\mathbf{11}^+$ (B3LYP/LANL2DZ in plain text and B3LYP/LANL2DZp in bold).

Energetic evidence for metal–metal interactions in ReC_xMn systems

To energetically quantify the rhenium–manganese interactions, homodesmotic equations[21] were employed. These have been widely and successfully used in organic systems. Endothermicity implies that destabilizing interactions dominate, and exothermicity implies that stabilizing interactions dominate.[22] Thermoneutrality implies a balance (not an absence) of such interactions. The charge and mass-balanced equilibria in Scheme 3 were investigated, with the monometallic complexes and organocumulenes as reference compounds.

As shown in Scheme 3, there is a stabilizing rhenium–manganese interaction in $\mathbf{8}^+$ of 20.3 kcal mol^{-1} at the B3LYP/LANL2DZ level, and 22.5 kcal mol^{-1} at the more accurate B3LYP/LANL2DZp level. In view of the reasonable agreement, the former was used for higher homologs. This interaction attenuates strongly with increased chain length: a decrease of 6.3 kcal mol^{-1} or 31.0% between $\mathbf{8}^+$ and $\mathbf{9}^+$; a decrease of 2.8 kcal mol^{-1} or 20.0% between $\mathbf{9}^+$ and $\mathbf{10}^+$; a decrease of 1.8 kcal mol^{-1} or 16.1% between $\mathbf{10}^+$ and $\mathbf{11}^+$. As would be intuitively expected, studies generally show a reduction of electronic interactions as unsaturated bridges are extended.[2e,23] Nonetheless, our data suggest a non-zero macromolecular limit. Fig. 6 presents a variant of the classical Lewis–Calvin plot,[24] in which an observable is graphed against the reciprocal of the carbon chain length, $1/x$. Extrapolation to $1/x = 0$ gives one estimate of the value at infinite chain length. The homodesmotic energies show a strikingly linear relationship, with a stabilization of −4 kcal mol^{-1} predicted for the C_∞ species.

A number of control experiments were conducted.[25,26] For example, the magnitudes of the stabilization energies depend upon the chain lengths of the monometallic reference complexes employed. However, equivalent relationships were always realized.

Unknown ReC_xRe, MnC_xMn and ReC_xMn systems

Motivated by the above results, we sought to investigate a family of complexes that are still unknown experimentally. One goal was to probe the dependence of the homodesmotic

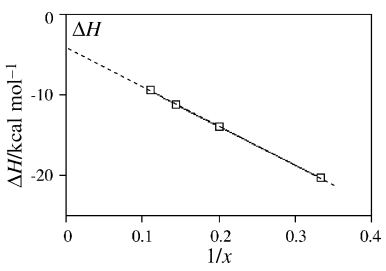

Fig. 6 Relationship between homodesmotic energies (Δ*H*, Scheme 3) and the reciprocal carbon chain length ($1/x$) of $\mathbf{8}^+$–$\mathbf{11}^+$.

energies upon the heterometallic *vs.* homometallic nature of a complex. Another was to probe for intrinsic differences in otherwise identical rhenium and manganese systems. Hence, complexes with the new endgroup $(\eta^5\text{-}C_5H_5)(CO)_2Re$ (abbreviated Re′) were studied.

Calculations analogous to those in Fig. 1 and 3 were conducted on bimetallic complexes with identical endgroups, $(\eta^5\text{-}C_5H_5)(CO)_2MC_3M(CO)_2(\eta^5\text{-}C_5H_5)$ (M = Re, **12**; Mn, **13**), and related complexes with dissimilar endgroups, $(\eta^5\text{-}C_5H_5)(CO)_2ReC_3Mn(CO)_2(\eta^5\text{-}C_5H_5)$ (**14**) and $[(\eta^5\text{-}C_5H_5)(NO)(PH_3)ReC_3Re(CO)_2(\eta^5\text{-}C_5H_5)]^+$ ($\mathbf{15}^+$). Data are summarized in Fig. 7. Metrical parameters were nearly identical at the B3LYP/LANL2DZ and B3LYP/LANL2DZp levels. Analogous calculations for the monometallic allenylidene reference complexes ($\mathbf{MnC_3H_2}$ and $\mathbf{Re'C_3H_2}$) are given in Fig. 3 and 7, respectively. NBO-derived data for all of these species are given in Table 3.

As depicted in Fig. 7, **12** and **13** exhibit C_2 symmetry, with CpReReCp and CpMnMnCp torsion-type angles of 104.8 and 94.0°. The heterobimetallic complex **14** adopts an analogous conformation (CpMnReCp = 104.1°). These near-orthogonal endgroup orientations follow readily from the HOMOs of the $(\eta^5\text{-}C_5H_5)(CO)_2M$ fragments shown in Fig. 2. The cationic dirhenium complex $\mathbf{15}^+$ adopts a conformation analogous to that of the rhenium–manganese analog $\mathbf{8}^+$.

Complex $\mathbf{15}^+$ also exhibits similar metal–metal interactions. For example, the (H_3P)Re–C and (OC)Re–C bond lengths differ significantly (1.946 *vs.* 1.856 Å, Fig. 7). The former is longer than that in the monorhenium reference compound $[\mathbf{ReC_3H_2}]^+$ (1.913 Å, Fig. 3), and the latter is shorter than that in $\mathbf{Re'C_3H_2}$ (1.913 Å, Fig. 7). Both reference compounds exhibit virtually identical Re=C bond lengths and bond orders (Table 3), emphasizing that the linkages in $\mathbf{15}^+$ must have a substantially altered bonding nature. Indeed, the NBO protocol indicates a new type of dominant resonance form, a Re–C≡C–C≡Re^+ or alkynyl/carbyne species. The (OC)Re≡C triple bond character is evidenced by the shortest Re–C distance and the highest NLMO bond order (1.438, Table 3) of any of the preceding compounds, and two orthogonal sets of CRe′ orbital coefficients with appreciable magnitudes at carbon (61.9 and 28.2%; 67.0 and 21.8%). The difference between $\mathbf{15}^+$ and $\mathbf{8}^+$ can be rationalized from the greater π donor strength of rhenium *vs.* analogous manganese fragments. Comparison of the natural charges of the endgroups with those of the monorhenium reference compounds shows a charge transfer of magnitude 0.187 through the C_3 chain, in the direction from (H_3P)Re (Re) to (OC)Re (Re′). However, note that the natural charge of the former endgroup remains greater (0.787 *vs.* 0.487), despite the formal positive charge on the rhenium of the latter in the dominant resonance form.

In contrast, the NBO data show the more symmetrical complexes **12**–**14** to have fully cumulated M=C=C=C=M linkages. The bond orders and carbon p orbital coefficients associated with the Re=C bonds are always slightly higher than those of the Mn=C bonds (1.295–1.252 *vs.* 0.907–0.900; 21.0–20.9 *vs.* 17.1–16.5%). The endgroups of these neutral complexes exhibit much lower natural charges, with essentially neutral carbon chains. Also, the magnitude of charge transfer in the unsymmetrical compound **14** (0.075 from rhenium to manganese) is less than half that of $\mathbf{8}^+$ and $\mathbf{15}^+$.

To quantify the relative metal–metal interactions in **12**–**14**, the homodesmotic equations in Scheme 4 (top) were employed. The B3LYP/LANL2DZp data show an essentially constant interaction energy (−21.4 to −22.2 kcal mol^{-1}), independent of the metal. Complex $\mathbf{15}^+$ gives an interaction energy (Scheme 4, bottom) very similar to that of $\mathbf{8}^+$ (Scheme 3). Hence, the substitution of $\mathbf{MnC_3H_2}$ by $\mathbf{Re'C_3H_2}$ has only a small effect in all homodesmotic systems examined.

Analogous calculations were conducted for the corresponding homo- and heterobimetallic C_5 complexes (**16**–**18**, $\mathbf{19}^+$). The optimized geometries at the B3LYP/LANL2DZ level are given in Fig. 8, and the homodesmotic energies are summarized in Scheme 4. The latter were again nearly independent of the metal, but diminished to −13.9 to −14.4 kcal mol^{-1}. Based upon the data in Scheme 3, the C_7 and C_9 homologs of **12**–**14** and $\mathbf{15}^+$ should exhibit further, parallel decreases.

Structures and thermodynamics of ReC_3W systems

The heterobimetallic rhenium/tungsten C_3 complex $(\eta^5\text{-}C_5Me_5)(NO)(PPh_3)ReC{\equiv}CC{\equiv}W(O\text{-}t\text{-}Bu)_3$ (**7**) shown in Scheme 2 was prepared by stoichiometric triple bond metatheses of diynyl complexes $(\eta^5\text{-}C_5Me_5)(NO)(PPh_3)ReC{\equiv}CC{\equiv}CR$ (R = H, Me) and $(t\text{-}BuO)_3W{\equiv}W(O\text{-}t\text{-}Bu)_3$.[6] In contrast to $\mathbf{4}^+BF_4^-$, **7** carries no formal charge. It crystallized as an alkoxy-bridged tungsten dimer, a motif found for many but by no means all $X{\equiv}W(OR)_3$ systems.

Table 3 Natural charge, bond hybridization (orbital coefficients) and NLMO bond order data (B3LYP/LANL2DZp)

	12 ($\mathbf{Re'C_3Re'}$)	**13** ($\mathbf{MnC_3Mn}$)	**14** ($\mathbf{Re'C_3Mn}$)	$\mathbf{15}^+$ ($[\mathbf{ReC_3Re'}]^+$)	$\mathbf{Re'C_3H_2}$
Natural charge					
$^{\delta}M$	0.068/Re′[a]		0.082/Re′[a]	0.487/Re′[a]	0.113/Re′[a]
		−0.048/Mn[b]	−0.064/Mn[b]	0.787/Re[c]	
$\Delta(^{\delta}M - {}^{\delta}C)$[d]	0.151/Re–C		0.162/Re–C	0.162/Re–C	0.045/Re–C
		0.783/Mn–C	0.772/Mn–C	0.079/Re–C	
Hybridization (orbital coefficients)					
M–C/σ	$s^1d^{6.20}$ (Re, 35.3%)		$s^1d^{8.25}$ (Re, 39.7%)	$s^1d^{8.99}$ (Re, 37.2%)	$s^1d^{5.77}$ (Re, 34.2%)
	$s^1p^{0.96}$ (CRe, 62.7%)		$s^1p^{0.98}$ (CRe, 59.0%)	$s^1p^{1.03}$ (CRe, 61.4%)	$s^1p^{0.99}$ (CRe, 63.3%)
		$s^1d^{6.89}$ (Mn, 34.6%)	$s^1d^{7.05}$ (Mn, 35.1%)	$s^1d^{7.19}$ (Re′, 37.7%)	
		$s^1p^{0.86}$ (CMn, 61.5%)	$s^1p^{0.87}$ (CMn, 61.1%)	$s^1p^{0.97}$ (CRe′, 60.7%)	
M–C/π	d(Re, 67.7%)		d(Re, 68.0%)	d(Re′, 61.9%)	d(Re, 62.0%)
	p(CRe, 20.9%)		p(CRe, 21.0%)	p(CRe′, 28.2%)	p(CRe, 26.3%)
		d(Mn, 73.6%)	d(Mn, 73.8%)	d(Re′, 67.0%)	
		p(CMn, 17.1%)	p(CMn, 16.5%)	$s^1p^{11.22}$ (CRe′, 21.8%)	
Lone pair interactions				d(Re, 82.0%)[e]	
				p(CRe, 8.3%)	
NLMO	1.252/Re–C		1.295/Re–C	0.865/Re–C	1.098/Re–C
		0.907/Mn–C	0.900/Mn–C	1.438/Re′–C	

[a] The $(\eta^5\text{-}C_5H_5)(CO)_2Re$ endgroup. [b] The $(\eta^5\text{-}C_5H_5)(CO)_2Mn$ endgroup. [c] The $(\eta^5\text{-}C_5H_5)(NO)(PH_3)Re$ endgroup. [d] The charge difference between metal and the first chain carbon. [e] The d-type lone pair on rhenium with partial occupation of 1.63 electrons.

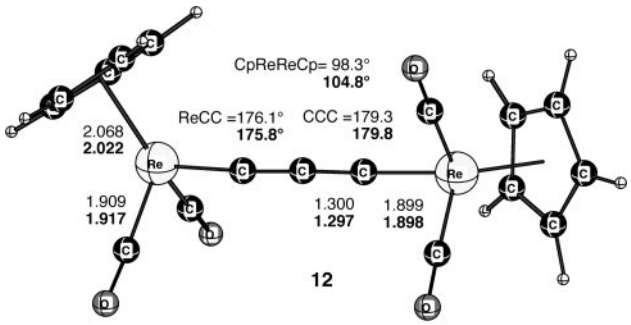

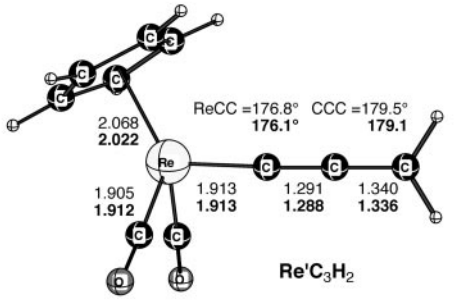

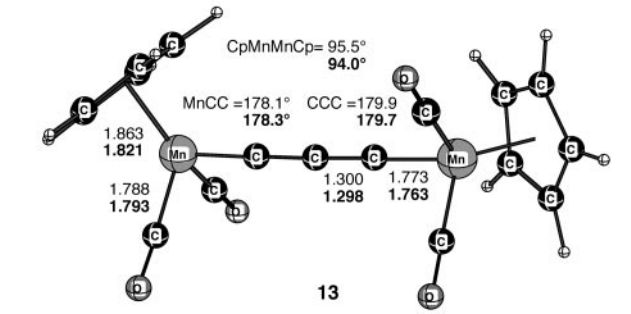

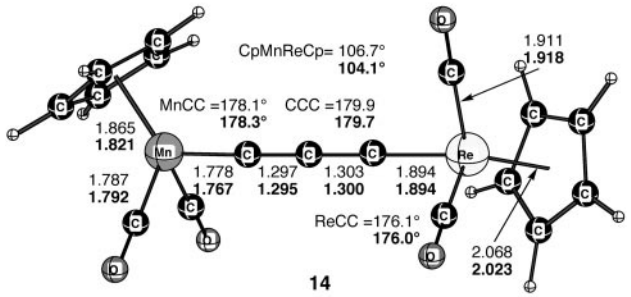

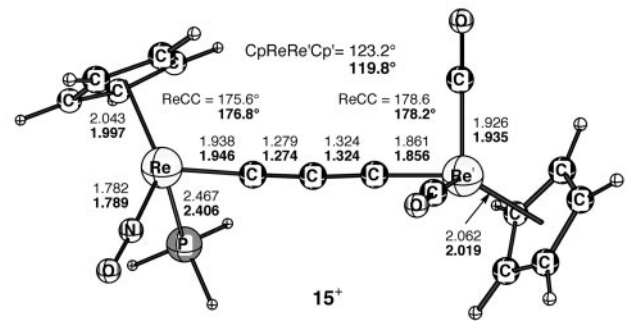

Fig. 7 Computed bond lengths (Å) and angles (deg) for (η^5-C_5H_5)$(CO)_2$M(1)C_3M(2)$(CO)_2(\eta^5$-C_5H_5) [M(1)/M(2) = Re/Re, **12**; Mn/Mn, **13**; Re/Mn, **14**], (η^5-C_5H_5)$(CO)_2$ReC_3H_2 (**Re′C_3H_2**) and [(η^5-C_5H_5)(NO)(PH_3)ReC_3Re$(CO)_2(\eta^5$-C_5H_5)]$^+$ (**15**$^+$) (B3LYP/LANL2DZ in plain text and B3LYP/LANL2DZp in bold).

The geometries of the model compounds (η^5-C_5H_5)-(NO)(PH_3)ReC≡CC≡W$(OMe)_3$ (**21**) and $(MeO)_3$W≡ W$(OMe)_3$ (**22**) were optimized at the B3LYP/LANL2DZp level and the results are summarized in Fig. 9. Both agree well with the

$$(\eta^5\text{-}C_5H_5)(CO)_2M(1)C_xH_2 + (\eta^5\text{-}C_5H_5)(CO)_2M(2)C_xH_2 = H_2C_xH_2 + (\eta^5\text{-}C_5H_5)(CO)_2M(1)C_xM(2)(CO)_2(\eta^5\text{-}C_5H_5)$$

$x = 3$
$\Delta H = \mathbf{-22.2}/-22.7$ (**12**, Re/Re)
$\Delta H = \mathbf{-21.4}/-22.1$ (**13**, Mn/Mn)
$\Delta H = \mathbf{-21.9}/-22.6$ (**14**, Re/Mn)

$x = 5$
$\Delta H = -14.4$ (**16**, Re/Re)
$\Delta H = -13.9$ (**17**, Mn/Mn)
$\Delta H = -14.3$ (**18**, Re/Mn)

$$Re'C_xH_2 + [ReC_xH_2]^+ = H_2C_xH_2 + [(\eta^5\text{-}C_5H_5)(NO)(PH_3)ReC_xRe(CO)_2(\eta^5\text{-}C_5H_5)]^+$$

$\Delta H = \mathbf{-25.2}/-22.9$ ($x = 3$, **15**$^+$)
$\Delta H = -16.5$ ($x = 5$, **19**$^+$)

Scheme 4 Homodesmotic energies (kcal mol^{-1}) for **12–14**, **15**$^+$, **16–18** and **19**$^+$ (B3LYP/LANL2DZp in plain text and B3LYP/LANL2DZp in bold).

X-ray structures of the real systems.[6,27] The linearity of the ReC_3W linkage is indicated by the ReCC (176.9°), CCC (178.8°) and CCW (179.9°) bond angles. To help define other properties, analogous calculations were conducted with the

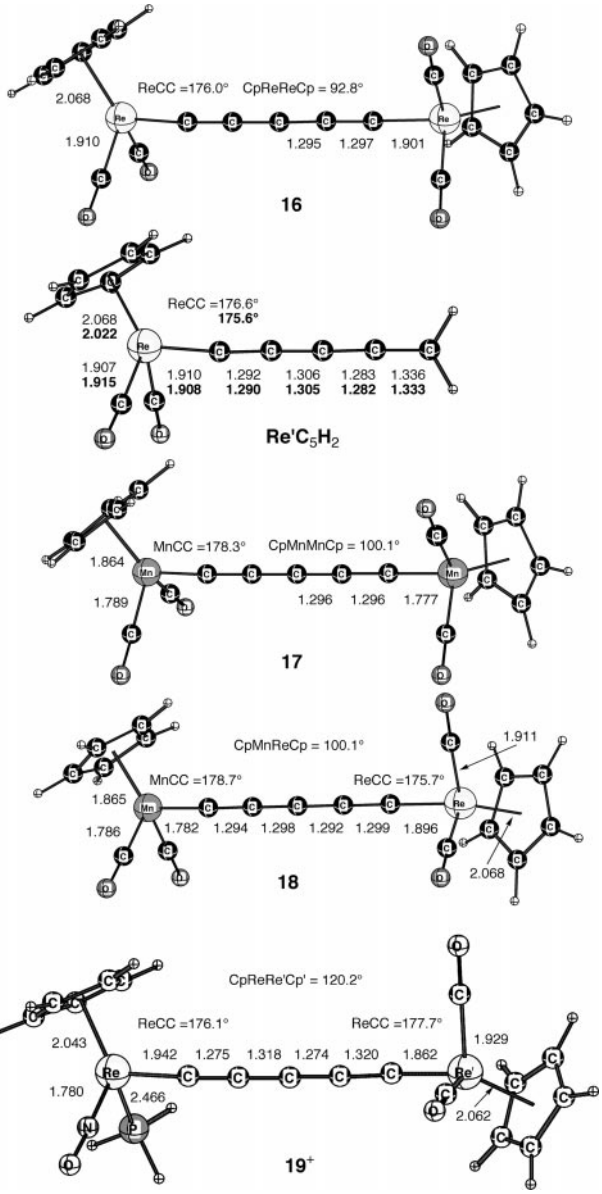

Fig. 8 Computed bond lengths (Å) and angles (deg) for (η^5-C_5H_5)$(CO)_2$M(1)C_3M(2)$(CO)_2(\eta^5$-C_5H_5) [M(1)/M(2) = Re/Re, **16**; Mn/Mn, **17**; Re/Mn, **18**], (η^5-C_5H_5)$(CO)_2$ReC_5H_2 (**Re′C_5H_2**) and [(η^5-C_5H_5)(NO)(PH_3)ReC_5Re$(CO)_2(\eta^5$-C_5H_5)]$^+$ (**19**$^+$) (B3LYP/LANL2DZ in plain text and B3LYP/LANL2DZp in bold).

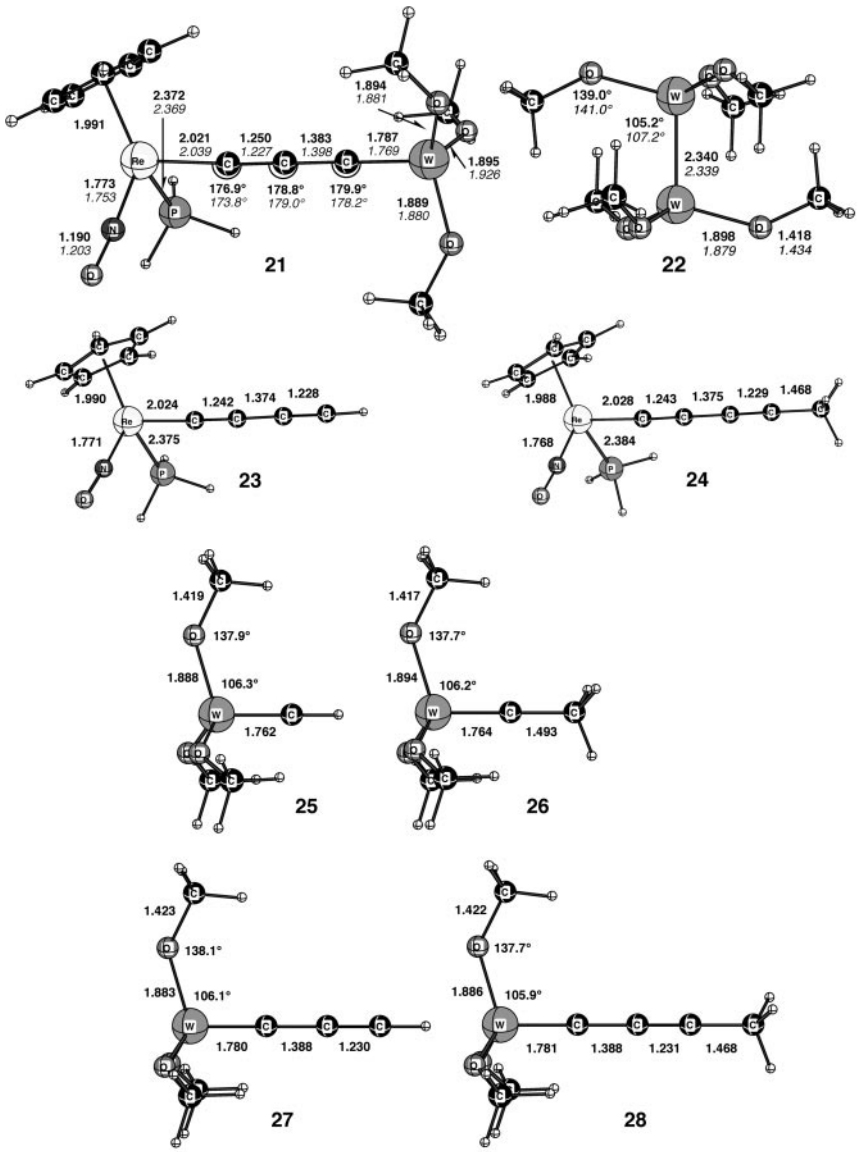

Fig. 9 Computed bond lengths (Å) and angles (deg) for $(\eta^5\text{-}C_5\underline{H}_5)(NO)(P\underline{H}_3)ReC_3W(O\underline{Me})_3$ (**21**), $(MeO)_3W{\equiv}W(OMe)_3$ (**22**), $(\eta^5\text{-}C_5H_5)$-$(NO)(PH_3)ReC{\equiv}CC{\equiv}CR$ (R = H, **23**; Me, **24**) and $(MeO)_3W{\equiv}CR$ (R = H, **25**; Me, **26**; C≡CH, **27**; C≡CMe, **28**) (B3LYP/LANL2DZp in bold), and a comparison to the X-ray data (italics) for **7** (Scheme 2) and $(t\text{-}BuO)_3W{\equiv}W(O\text{-}t\text{-}Bu)_3$.

monometallic reference complexes $(\eta^5\text{-}C_5H_5)(NO)(PH_3)$-$ReC{\equiv}CC{\equiv}CR$ (R=H, **23**; Me, **24**) and $(MeO)_3W{\equiv}CR$ (R = H, **25**; Me, **26**; C≡CH, **27**; C≡CMe, **28**).

The total electronic energies of all complexes are summarized in Table 1. From these, it is a simple matter to compute the enthalpies for the triple bond metatheses in Scheme 5 [eqn. (1), top]. In accord with the preparative experiments, both are exothermic.

The $ReC{\equiv}CC{\equiv}W$ bond lengths computed for **21** are essentially identical to those of the monometallic reference complexes. For example, the Re–C bond (2.021 Å) is very close to that of **24** (2.028 Å), and in accord with experimental data for closely related species.[17] The W≡C bond (1.787 Å) is also close to that of **28** (1.781 Å), and in agreement with experimental data for related alkoxy-bridged systems.[28] The ReC≡C and C–CW bonds (1.250 and 1.383 Å) closely match those of **24** and **28** (1.243 Å and 1.388 Å).

$$(\eta^5\text{-}C_5H_5)(NO)(PH_3)ReC{\equiv}CC{\equiv}CR + (MeO)_3W{\equiv}W(OMe)_3 = (\eta^5\text{-}C_5H_5)(NO)(PH_3)ReC{\equiv}CC{\equiv}W(OMe)_3\,(\mathbf{21}) + (MeO)_3W{\equiv}CR$$

$$\Delta H = -11.2 \text{ kcal mol}^{-1} \text{ (R = H)}$$
$$\Delta H = -8.6 \text{ kcal mol}^{-1} \text{ (R = Me)} \quad (1)$$

$$(\eta^5\text{-}C_5H_5)(NO)(PH_3)ReC{\equiv}CC{\equiv}CR + (MeO)_3W{\equiv}CC{\equiv}CR = (\eta^5\text{-}C_5H_5)(NO)(PH_3)ReC{\equiv}CC{\equiv}W(OMe)_3\,(\mathbf{21}) + RC{\equiv}CC{\equiv}CR$$

$$\Delta H = 1.46 \text{ kcal mol}^{-1} \text{ (R = H)}$$
$$\Delta H = 0.0 \text{ kcal mol}^{-1} \text{ (R = Me)} \quad (2)$$

Scheme 5 Metathesis [eqn. (1)] and homodesmotic [eqn. (2)] energies for **21** (B3LYP/LANL2DZp).

NBO results are summarized in Table 4. The data show the Re–C and W≡C linkages in **21** to have dominant single and triple bond character, with bond orders of 0.750 and 2.367. The monometallic reference compounds **24** and **28** give very similar values (0.708, 2.345). The rhenium endgroup in **21** has nearly the same natural charge as that in **24** (0.434 *vs.* 0.448), while the tungsten endgroup is only slightly less positive than in **28** (0.411 *vs.* 0.488). The electrostatic polarizations $[\Delta(^{\delta}M - {}^{\delta}C)]$ are also quite similar. In contrast to the situations with $\mathbf{8}^+$ and $\mathbf{15}^+$, both endgroups have similar positive charges (0.434 *vs.* 0.411), which furthermore indicates for this neutral compound a negatively charged chain. Also, there is only a slight amount of ground state charge transfer from rhenium to tungsten (0.023 *vs.* 0.166 and 0.180 for $\mathbf{8}^+$ and $\mathbf{15}^+$).

The enthalpies of the homodesmotic reactions in Scheme 5 [eqn. (2)] were calculated. In accord with the geometric and

Table 4 Natural charge, bond hybridization (orbital coefficients) and NLMO bond order data (B3LYP/LANL2DZp)

	21 (ReC_3W)	**24** (ReC_4Me)	**28**(WC_3Me)
Natural charge			
$^{\delta}M$	0.434/Re[a]	0.448/Re[a]	
	0.411/W[b]		0.488/W[b]
$\Delta(^{\delta}M - {}^{\delta}C)$[c]	0.430/Re–C	0.438/Re–C	
	2.090/W–C		2.132/W–C
Hybridization (orbital coefficients)			
M–C/σ	$s^1d^{6.43}$ (Re, 35.2%)	$s^1d^{6.62}$ (Re, 34.9%)	
	$s^1p^{1.14}$ (CRe, 62.4%)	$s^1p^{1.13}$ (CRe, 62.6%)	
	$s^1d^{5.94}$ (W, 33.4%)		$s^1d^{4.57}$ (W, 31.8%)
	$s^1p^{0.89}$ (CW, 66.0%)		$s^1p^{0.87}$ (CW, 67.1%)
M–C/π	d(W, 50.6; 47.6%)		d(W, 48.2; 48.0%)
	p(CW, 45.0; 46.7%)		p(CW, 46.8; 6.9)
NLMO	0.750/Re–C	0.708/Re–C	
bond order	2.367/W–C		2.345/W–C

[a] The $(\eta^5\text{-}C_5H_5)(NO)(PH_3)Re$ endgroup. [b] The $(MeO)_3W$ endgroup. [c] The charge difference between metal and the first chain carbon.

electronic properties, there is no evidence for any stabilizing (or destabilizing) interaction involving the rhenium and tungsten endgroups in **21**. These reactions constitute triple bond metatheses, and can in principle be experimentally evaluated. Scheme 5 poses an obvious question: why are the metatheses in eqn. (1) exothermic, but those in eqn. (2) not? It can be risky to interpret such differences in terms of a single factor. However, one possibility is that repulsive interactions associated with the W≡W linkage in **22** [unique to eqn. (1)] are relieved in the monotungsten products.

As with **7**,[6] $(t\text{-}BuO)_3W{\equiv}CMe$ crystallizes as a centrosymmetric dimer featuring trigonal bipyramidal tungsten atoms joined by equatorial/axial bridging *t*-butoxy ligands.[26] Hence, the dimerization of the model compound $(MeO)_3W{\equiv}CH$ (**25**) was studied. At the B3LYP/LANL2DZ level, the C_{2h} symmetrical dimer (**29**) is an energy minimum. As shown in Fig. 10, the B3LYP/LANL2DZp optimized structural parameters are close to the experimental X-ray data. The computed dimerization enthalpy was −14.6 kcal mol^{-1} (B3LYP/LANL2DZp corrected after ZPE at B3LYP/LANL2DZ).

Conclusions

Structure, bonding, and metal–metal interactions in a set of bimetallic complexes with bridging odd-carbon chains have been investigated by high level density functional theory computations. At the B3LYP/LANL2DZp level, the experimental structural parameters are reproduced very well. The structural, bond order, natural charge, and homodesmotic enthalpic data provide unambiguous evidence for marked metal–metal interactions in all model compounds for the real rhenium/manganese system $\mathbf{4}^+BF_4^-$. These include: (1) the series $\mathbf{8}^+$, $\mathbf{9}^+$, $\mathbf{10}^+$ and $\mathbf{11}^+$, in which the chain is extended, (2) the dirhenium analogs $\mathbf{15}^+$ and $\mathbf{19}^+$, and (3) the macromolecular limit of the one-dimensional carbon allotrope carbyne.[2e,29] Here, Fig. 6 suggests a reduced but still finite homodesmotic interaction energy. On the experimental side, the strong visible absorptions that characterize $\mathbf{4}^+BF_4^-$ and related compounds also deserve emphasis. These have molar extinction coefficients in the 50 000–100 000 M^{-1} cm^{-1} range, and there is good evidence for appreciable rhenium-to-manganese charge transfer character.[2d]

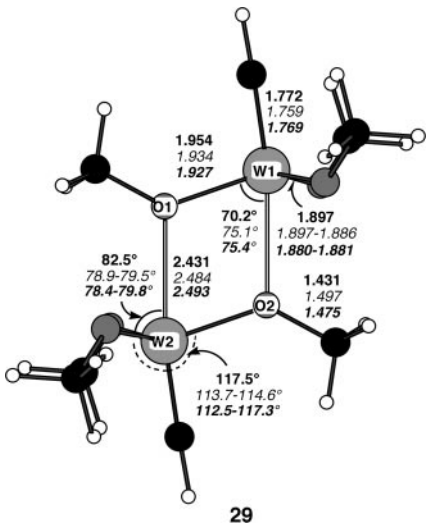

29

Fig. 10 Computed bond lengths (Å) and angles (°) for the dimer (**29**) of $(MeO)_3W{\equiv}CH$ (**25**) (B3LYP/LANL2DZp in bold), compared to the X-ray data for the dimer of $(t\text{-}BuO)_3W{\equiv}CMe$ (italics) and **7** (Scheme 2, bold italics).

The same features are found computationally for the three neutral complexes **12**, **13** and **14**, which presently have no experimental counterpart. We believe that the NBO-derived conclusion of dominant M=C=C=C=M character for these compounds, dominant $^+$Re–C=C=C=Mn character for $\mathbf{8}^+$, and dominant Re–C≡C–C≡Re^+ character for $\mathbf{15}^+$, is best regarded as a relative trend. A $^+$Re=C interaction clearly plays a conformation-determining role in the real system $\mathbf{4}^+BF_4^-$ [Fig. 2(C)]—which furthermore features a more electron-releasing pentamethylcyclopentadienyl ligand—and other experimental or theoretical probes may draw different dividing lines. This same point can be made with respect to the cationic chiral monorhenium compounds such as $[\mathbf{ReC_3H_2}]^+$—all of which have dominant $^+$Re=C character—and $\mathbf{8}^+$ and $\mathbf{15}^+$. We find this relative trend to be intuitively plausible (increasing π basicity of one terminus), but intensive efforts to find a "single parameter explanation" for the difference between **12**–**14** and $\mathbf{8}^+$ have not yet been successful.

In contrast to the case with $\mathbf{4}^+BF_4^-$, the structural, bond order, natural charge, and homodesmotic enthalpic data provide no evidence for significant metal–metal interactions in model compounds for the real rhenium/tungsten system **7**. Our efforts to find a single parameter explanation for this difference have also not been fruitful. Nonetheless, some patterns are apparent. For example, **7** does not exhibit any pronounced UV-visible absorptions and all features have counterparts in monometallic analogs. Also, despite the lack of overall charge, the model compound **21** shows substantial positive charge on each endgroup, such that the carbon chain carries nearly a full negative charge. Importantly, the data for $\mathbf{15}^+$ show that a dominant M–C≡C–C≡M resonance form does not "turn off" metal–metal interactions. Finally, close relatives of the ditungsten and monotungsten model compounds in Fig. 9 catalyze

triple bond metatheses,[30] and our structural, electronic, and enthalpic data provide—as an unintended corollary—a valuable foundation for further research in this area.

In summary, this study has provided a paradigm for the computational investigation of metal–metal interactions across sp carbon chains. It represents the first examination of odd-carbon systems and contains a variety of reference values that will aid future work. The data complement earlier elegant studies by Halet, Sgamellotti, and their collaborators of even-carbon chain complexes with ruthenium and iron endgroups.[4b,9] Extensions of this work to even-carbon chain complexes with rhenium endgroups will be described in subsequent publications.[12]

Acknowledgement

We thank the Deutsche Forschungsgemeinschaft (DFG; GL 300/2-1) for support.

References and notes

1 Recent reviews covering selected aspects of this field: (*a*) M. Akita and Y. Moro-oka, *Bull. Chem. Soc. Jpn.*, 1995, **68**, 420; (*b*) M. I. Bruce, *Coord. Chem. Rev.*, 1997, **166**, 91; (*c*) H. Werner, *Chem. Commun.*, 1997, 903; (*d*) F. Paul and C. Lapinte, *Coord. Chem. Rev.*, 1998, **178–180**, 427; (*e*) see also: *J. Organomet. Chem.*, 1999, **578**, a volume that is devoted to carbon-rich organometallics.

2 Full papers from our laboratory with extensive literature background: (*a*) W. Weng, T. Bartik, M. Brady, B. Bartik, J. A. Ramsden, A. M. Arif and J. A. Gladysz, *J. Am. Chem. Soc.*, 1995, **117**, 11922; (*b*) M. Brady, W. Weng, Y. Zhou, J. W. Seyler, A. J. Amoroso, A. M. Arif, M. Böhme, G. Frenking and J. A. Gladysz, *J. Am. Chem. Soc.*, 1997, **119**, 775; (*c*) S. B. Falloon, S. Szafert, A. M. Arif and J. A. Gladysz, *Chem. Eur. J.*, 1998, **4**, 1033; (*d*) T. Bartik, W. Weng, J. A. Ramsden, S. Szafert, S. B. Falloon, A. M. Arif and J. A. Gladysz, *J. Am. Chem. Soc.*, 1998, **120**, 11071; (*e*) R. Dembinski, T. Bartik, B. Bartik, M. Jaeger and J. A. Gladysz, *J. Am. Chem. Soc.*, 2000, **122**, 810.

3 (*a*) N. Le Narvor, L. Toupet and C. Lapinte, *J. Am. Chem. Soc.*, 1995, **117**, 7129; (*b*) F. Coat, M.-A. Guillevic, L. Toupet, F. Paul and C. Lapinte, *Organometallics*, 1997, **16**, 5988; (*c*) N. Le Narvor and C. Lapinte, *C. R. Acad. Sci., Sér. IIc: Chim.*, 1998, 745; (*d*) M. Guillemot, L. Toupet and C. Lapinte, *Organometallics*, 1998, **17**, 1928; (*e*) F. Coat, M. Guillemot, F. Paul and C. Lapinte, *J. Organomet. Chem.*, 1999, **578**, 76; (*f*) V. Guillaume, V. Mahias, A. Mari and C. Lapinte, *Organometallics*, 2000, **19**, 1422.

4 (*a*) M. I. Bruce, L. I. Denisovich, P. J. Low, S. M. Peregudova and N. A. Ustynyuk, *Mendeleev Commun.*, 1996, 200; (*b*) M. I. Bruce, P. J. Low, K. Costuas, J.-F. Halet, S. P. Best and G. A. Heath, *J. Am. Chem. Soc.*, 2000, **122**, 1949.

5 (*a*) B. E. Woodworth and J. L. Templeton, *J. Am. Chem. Soc.*, 1996, **118**, 7418; (*b*) Tp′ = hydridotris(3,5-dimethylpyrazolyl) borate.

6 R. Dembinski, S. Szafert, P. Haquette, T. Lis and J. A. Gladysz, *Organometallics*, 1999, **18**, 5438.

7 Other lead papers from 1999–2000 to a now extensive literature: (*a*) S. Kheradmandan, K. Heinze, H. W. Schmalle and H. Berke, *Angew. Chem.*, 1999, **111**, 2412; S. Kheradmandan, K. Heinze, H. W. Schmalle and H. Berke, *Angew. Chem., Int. Ed.*, 1999, **38**, 2270; (*b*) A. Sakurai, M. Akita and Y. Moro-oka, *Organometallics*, 1999, **18**, 3241; (*c*) T. B. Peters, J. C. Bohling, A. M. Arif and J. A. Gladysz, *Organometallics*, 1999, **18**, 3261; (*d*) M. I. Bruce, B. C. Hall, B. D. Kelly, P. J. Low, B. W. Skelton and A. H. White, *J. Chem. Soc., Dalton Trans.*, 1999, 3719; (*e*) S. Mihan, K. Sünkel and W. Beck, *Chem. Eur. J.*, 1999, **5**, 745; (*f*) E. Campazzi, E. Solari, R. Scopelliti and C. Floriani, *Chem. Commun.*, 1999, 1617; (*g*) J. Gil-Rubio, M. Laubender and H. Werner, *Organometallics*, 2000, **19**, 1365; (*h*) F. Paul, W. E. Meyer, L. Toupet, H. Jiao, J. A. Gladysz and C. Lapinte, *J. Am. Chem. Soc.*, 2000, **122**, 9405.

8 M. I. Bruce, J.-F. Halet, S. Kahlal, P. J. Low, B. W. Skelton and A. H. White, *J. Organomet. Chem.*, 1999, **578**, 155.

9 (*a*) P. Belanzoni, N. Re, M. Rosi, A. Sgamellotti and C. Floriani, *Organometallics*, 1996, **15**, 4264; (*b*) P. Belanzoni, N. Re, A. Sgamellotti and C. Floriani, *J. Chem. Soc., Dalton Trans.*, 1997, 4773; (*c*) P. Belanzoni, N. Re, A. Sgamellotti and C. Floriani, *J. Chem. Soc., Dalton Trans.*, 1998, 1825; (*d*) N. Re, A. Sgamellotti and C. Floriani, *J. Chem. Soc., Dalton Trans.*, 1998, 2521; (*e*) P. Belanzoni, A. Sgamellotti, N. Re and C. Floriani, *Inorg. Chem.*, 2000, **39**, 1147.

10 (*a*) T. F. Miller and M. B. Hall, *J. Am. Chem. Soc.*, 1999, **121**, 7389; (*b*) S. T. Brown, J. C. Rienstra-Kiracofe and H. F. Schaefer III, *J. Phys. Chem. A*, 1999, **103**, 4065; (*c*) A. I. Boldyrev and J. Simons, *J. Phys. Chem. A*, 1997, **101**, 2215; (*d*) F. Nunzi, A. Sgamellotti, N. Re and C. Floriani, *Organometallics*, 2000, **19**, 1628.

11 see also: (*a*) J. Le Bras, H. Jiao, W. E. Meyer, F. Hampel and J. A. Gladysz, *J. Organomet. Chem.*, 2000, **616**, 54; (*b*) W. Mohr, G. A. Stark, H. Jiao and J. A. Gladysz, *Eur. J. Inorg. Chem.*, 2001, 925.

12 H. Jiao and J. A. Gladysz, manuscript in preparation.

13 For other types of complexes with C_3 ligands, see ref. 2(*c*) and: (*a*) M. S. Morton and J. P. Selegue, *J. Organomet. Chem.*, 1999, **578**, 133; (*b*) S. B. Falloon, W. Weng, A. M. Arif and J. A. Gladysz, *Organometallics*, 1997, **16**, 2008.

14 M. J. Frisch, G. W. Trucks, H. B. Schlegel, G. E. Scuseria, M. A. Robb, J. R. Cheeseman, V. G. Zakrzewski, J. A. Montgomery, Jr., R. E. Stratmann, J. C. Burant, S. Dapprich, J. M. Millam, A. D. Daniels, K. N. Kudin, M. C. Strain, O. Farkas, J. Tomasi, V. Barone, M. Cossi, R. Cammi, B. Mennucci, C. Pomelli, C. Adamo, S. Clifford, J. Ochterski, G. A. Petersson, P. Y. Ayala, Q. Cui, K. Morokuma, D. K. Malick, A. D. Rabuck, K. Raghavachari, J. B. Foresman, J. Cioslowski, J. V. Ortiz, B. B. Stefanov, G. Liu, A. Liashenko, P. Piskorz, I. Komaromi, R. Gomperts, R. L. Martin, D. J. Fox, T. Keith, M. A. Al-Laham, C. Y. Peng, A. Nanayakkara, C. Gonzalez, M. Challacombe, P. M. W. Gill, B. Johnson, W. Chen, M. W. Wong, J. L. Andres, C. Gonzalez, M. Head-Gordon, E. S. Replogle and J. A. Pople, GAUSSIAN 98, Rev. A.5, Gaussian, Inc., Pittsburgh, PA, 1998; for computational methods and applications see: (*a*) W. J. Hehre, L. Radom, P. v. R. Schleyer and J. A. Pople, *Ab Initio Molecular Orbital Theory*, Wiley, New York, 1986; (*b*) J. B. Foresman and Æ. Frisch, *Exploring Chemistry with Electronic Structure Methods: A Guide to Using Gaussian*, 2nd edn., Gaussian, Inc., Pittsburgh, PA, 1996.

15 (*a*) P. J. Hay and W. R. Wadt, *J. Chem. Phys.*, 1985, **82**, 299; (*b*) T. H. Dunning, Jr. and P. J. Hay, *Modern Theoretical Chemistry*, ed. H. F. Schaefer III, Plenum, New York, 1976, p. 1. For polarization functions, see: S. Huzinaga, J. Anzelm, M. Klobukowski, E. Radzio-Andzelm, Y. Sakai and H. Tatewaki, *Gaussian Basis Sets for Molecular Calculations*, Elsevier, Amsterdam, 1984.

16 (*a*) E. D. Glendening, A. E. Reed, J. E. Carpenter and F. Weinhold, NBO Program, ver. 3.1, as implemented in link 607 of GAUSSIAN 98; (*b*) A. E. Reed, L. A. Curtiss and F. Weinhold, *Chem. Rev.*, 1988, **88**, 899.

17 Relevant experimental Re–C bond lengths: (*a*) $(\eta^5\text{-}C_5H_5)(NO)(PPh_3)Re(C{\equiv}CCH_3)$ and $[(\eta^5\text{-}C_5H_5)(NO)(PPh_3)Re\{{=}C{=}CH\text{-}(1\text{-naphthyl})\}]^+PF_6^-$: 2.066(7) and 1.841(17) Å from R. Senn, A. Wong, A. T. Patton, M. Marsi, C. E. Strouse and J. A. Gladysz, *J. Am. Chem. Soc.*, 1988, **110**, 6096; (*b*) $(\eta^5\text{-}C_5Me_5)(NO)(PPh_3)Re\{(C{\equiv}C)_nX\}$: 2.032(7) for $n/X = 4/SiMe_3$ from B. Bartik, R. Dembinski, T. Bartik, A. M. Arif and J. A. Gladysz, *New J. Chem.*, 1997, **21**, 739 and 1.998(12) and 2.016(8) Å for $n/X = 3/p\text{-}C_6H_4CH_3$ and $4/p\text{-}C_6H_4CH_3$ from R. Dembrinski, T. Lis, S. Szafert, C. L. Mayne, T. Bartik and J. A. Gladysz, *J. Organomet. Chem.*, 1999, **578**, 229.

18 H. Berke, G. v. Huttner and J. Seyerl, *Z. Naturforsch., B*, 1981, **36**, 1277.

19 S. Szafert, P. Haquette, S. B. Falloon and J. A. Gladysz, *J. Organomet. Chem.*, 2000, **604**, 52.

20 (*a*) D. Touchard, P. Haquette, A. Daridor, L. Toupet and P. H. Dixneuf, *J. Am. Chem. Soc.*, 1994, **116**, 11157; (*b*) G. Roth and H. Fischer, *Organometallics*, 1996, **15**, 1139 and 5766; (*c*) R. W. Lass, P. Steinert, J. Wolf and H. Werner, *Chem. Eur. J.*, 1996, **2**, 19; (*d*) I. Kovacik, M. Laubender and H. Werner, *Organometallics*, 1997, **16**, 5607.

21 P. Georg, M. Trachtman, C. W. Bock and A. M. Bret, *J. Chem. Soc., Perkin Trans. 2*, 1976, 1222. The term homodesmotic denotes reactions in which there are equal numbers of (1) each type of bond in reactants and products and (2) each type of atom with the same connections in reactants and products .

22 S. P. Verevkin, H.-D. Beckhaus, C. Rückhardt, R. Haag, S. I. Kozhushkov, T. Zywietz, A. de Meijere, H. Jiao and P. v. R. Schleyer, *J. Am. Chem. Soc.*, 1998, **120**, 11130. In homodesmotic reactions of the type A + B = C + D, the enthalpy correction at 0 K (ZPE) or finite temperatures is nearly negligible due to complete cancellation between the reactants and products (for examples, see: R. L. Disch and J. M. Schulman, *Chem. Phys. Lett.*,

1988, **152**, 402). Therefore, the enthalpies can be reliably approximated by reaction energies. This greatly reduces the computer resources needed for frequency calculations.

23 (*a*) G. U. Bublitz, R. Ortiz, S. R. Marder and S. G. Boxer, *J. Am. Chem. Soc*., 1997, **119**, 3365 and references therein; (*b*) A. Mishra, R. K. Behera, P. K. Behera, B. K. Mishra and G. B. Behera, *Chem. Rev*., 2000, **100**, 1973; (*c*) Y. Deng, G. Gao, H. He and L. D. Kispert, *J. Phys. Chem. B*, 2000, **104**, 5651.

24 (*a*) G. N. Lewis and M. Calvin, *Chem. Rev*., 1939, **25**, 273; (*b*) K. Knoll and R. R. Schrock, *J. Am. Chem. Soc*., 1988, **110**, 7989; (*c*) G. Schermann, T. Grösser, F. Hampel and A. Hirsch, *Chem. Eur. J*., 1997, **3**, 1105.

25 Energies for the following equations were calculated at the same level: $(\eta^5\text{-}C_5H_5)(CO)_2MnC_xH_2 + [(\eta^5\text{-}C_5H_5)(NO)(PH_3)\text{-}ReC_3H_2]^+ = H_2C_xH_2 + [(\eta^5\text{-}C_5H_5)(NO)(PH_3)ReC_3Mn\text{-}(CO)_2(\eta^5\text{-}C_5H_5)]^+$. Results: -16.6 kcal mol^{-1}, $x = 5$; -13.9 kcal mol^{-1}, $x = 7$.

26 Energies were also calculated at the same level with polyyne-type (instead of cumulenic) reference compounds: $[(\eta^5\text{-}C_5H_5)\text{-}(CO)_2Mn{\equiv}CC{\equiv}CMe]^+ + (\eta^5\text{-}C_5H_5)(NO)(PH_3)ReC{\equiv}CMe = [(\eta^5\text{-}C_5H_5)(NO)(PH_3)ReC_3Mn(CO)_2(\eta^5\text{-}C_5H_5)]^+ + MeC{\equiv}C\,C{\equiv}CMe$. Result: -30.2 kcal mol^{-1}.

27 M. H. Chisholm, K. Folting, M. Hampden-Smith and C. A. Smith, *Polyhedron*, 1987, **6**, 1747.

28 Other relevant W≡C bond lengths: (*a*) $(t\text{-}BuO)_3W{\equiv}CCH_3$: 1.759(6) Å from M. H. Chisholm, D. M. Hoffman and J. C. Huffman, *Inorg*. Chem., 1983, **22**, 2903; (*b*) $(t\text{-}BuO)_3W{\equiv}CNMe_2$: 1.77(2) Å from M. H. Chisholm, J. C. Huffman and N. S. Marchant, *J. Am. Chem. Soc*., 1983, **105**, 6162; (*c*) $(t\text{-}BuO)_3W{\equiv}CPh$: 1.758(5) Å from F. A. Cotton, W. Schwotzer and E. S. Shamshoum, *Organometallics*, 1984, **3**, 1770; (*d*) $(t\text{-}BuO)_3W{\equiv}C\text{-}p\text{-}C_6H_4R$; R = NMe_2/SMe, 1.754(7)/1.757(6) Å from H. A. Brison, T. P. Pollagi, T. C. Stoner, S. J. Geib and M. D. Hopkins, *Chem. Commun*., 1997, 1263.

29 (*a*) V. M. Mel'nichenko, A. M. Sladkov and Yu. N. Nikulin, *Russ. Chem. Rev*., 1982, **51**, 421; (*b*) P. P. K. Smith and P. R. Buseck, *Science*, 1982, **216**, 984; (*c*) Yu. P. Kudryavtsev, S. Evsyukov, M. Guseva, V. Babaev and V. Khvostov, *Chemistry and Physics of Carbon*, ed. P. A. Thrower, Marcel Dekker, New York, 1997; vol. 25, pp. 1–69; (*d*) J. Hlavaty, L. Kavan, N. Kasahara and A. Oya, *Chem. Commun*., 2000, 737.

30 U. H. F. Bunz and L. Kloppenburg, *Angew. Chem., Int. Ed*., 1999, **38**, 478; U. H. F. Bunz and L. Kloppenburg, *Angew. Chem*., 1999, **111**, 503.